Contents list available at IJRED website
International Journal of Renewable Energy Development
Journal homepage: https://ijred.undip.ac.id
Research Article

A bilevel zonal dispatch strategy considering electric vehicle users' demand response

Zhenya Ji[a,b], Yuyang Zhang[a], Zheng Wang[c], Lulu Liu[a], Hao Li[d*]

[a]School of Electrical and Automation Engineering, Nanjing Normal University, Nanjing, China
[b]International Joint Laboratory of Integrated Energy Equipment and Integration in Jiangsu Province, Nanjing, China
[c]State Grid Jiangsu Electric Vehicle Service Co., China
[d]CRRC Nanjing Puzhen Haitai Equipment Co., Ltd., Nanjing, China

Abstract. With the growing global energy crisis and environmental problems, the large-scale deployment of electric vehicles (EVs) and various types of distributed renewable energy sources has become an important measure to promote sustainable development in China's power sector. However, the rapid increase in the penetration rate of these distributed resources has gradually increased the operational pressure on distribution networks. To effectively address this issue, this paper proposes a two-layer partitioned optimization scheduling strategy for the distribution network layer and the aggregation layer, considering the price-based demand response of EV users. The upper distribution network layer focuses on its own low-carbon and economic operation, establishing a low-carbon economic optimization scheduling model for the distribution network layer to allocate global resources and formulate energy interaction strategies and constraints between aggregation areas based on this. The lower layer first constructs a comprehensive partitioning scheme considering the electrical distance between nodes, the dispatchable potential of EVs, and the power balance of distributed resources. Then, aiming at the economic operation of the aggregation area itself, it establishes a price-based demand response model for EV users to achieve optimal scheduling of distributed resources in the aggregation layer. This study aims to achieve the economic and low-carbon operation of distribution networks through reasonable scheduling strategies, while meeting the charging needs of EVs and improving the utilization efficiency of distributed resources. Simulation results show that the proposed two-layer scheduling strategy can effectively mobilize distributed resources in the distribution network to meet the needs of system economic operation. After optimization at the distribution network layer, the daily operating cost is reduced from 11,551.88 yuan to 6,220.84 yuan, significantly improving economic benefits. Electric vehicles have achieved a reduction of 21.1% in load peak shaving. In conclusion, the two-layer partitioned optimization scheduling strategy proposed in this paper can effectively utilize distributed resources in distribution networks, reduce operation costs, and achieve economic and low-carbon operation of distribution networks.

Keywords: Electric vehicles, Orderly charging, Multi-level adjustable charging, Different scenarios, Minimization of peak-to-valley difference

Received: 20th Feb 2025; Revised: 7th April 2025; Accepted: 30th April 2025; Available online: 8th May 2025

1. Introduction

With the widespread deployment of distributed power sources in distribution networks and the increasing penetration of new energy utilization devices (Adham *et al.*, 2025) such as electric vehicles (EVs) and distributed energy storages, traditional centralized control strategies face challenges such as large data detection volumes and high communication costs when uniformly scheduling all devices. The implementation of these strategies is quite difficult (Zhao *et al.*, 2023; Mousa *et al.*, 2024). Therefore, it is necessary to aggregate distributed devices into clusters and decompose the distribution network scheduling tasks into these clusters. Each cluster can then develop its own scheduling strategies to optimize the operation of local distributed devices, thereby achieving the overall economic and secure operation of the distribution network (Luo *et al.*, 2020). Many scholars have conducted research in this area.

Compared with traditional centralized scheduling methods, hierarchical and partitioned cluster scheduling requires coordination of the interests of multiple parties (Huang *et al.*, 2023). Shan *et al.*, (2023) considered the operational characteristics of equipment hardware and achieved a balance between system stability and economic efficiency through a three-layer control structure. However, the proposed control strategy is relatively rigid and does not sufficiently consider the autonomy of each layer. Feng *et al.*, (2023) took into account the interests of entities across multiple layers and balanced the interests of the distribution network and prosumers by establishing a cooperative game model. This model facilitated the full absorption of renewable energy and achieved profit distribution among participants. However, it treated EVs as fully compliant with scheduling, neglecting their autonomous charging behavior and response characteristics.

The growing public awareness of environmental concerns linked to vehicle emissions has accelerated the development of cleaner transportation options (Nguyen *et al.*, 2022; Tippichai *et al.*, 2023). In recent years, with the explosive growth in the number of EVs, their potential to bring significant economic benefits and low-carbon opportunities to distribution networks

* Corresponding author
Email: jizhenya@njnu.edu.cn (H.Li)

has attracted the attention of many scholars (Tian *et al.*, 2024; Teng *et al.*, 2024). The interaction technology between EVs and the grid has also developed rapidly, especially Vehicle-to-Grid (V2G) technology (Naqash *et al.*, 2021; Ahsan *et al.*, 2023; Yang *et al.*, 2024), which is an effective means to further exploit the potential of EVs. V2G aims to connect EVs to the distribution network through bidirectional power conversion devices, enabling two-way energy interaction between EVs and the distribution network. Statistical studies (Kempton *et al.*, 2005; Mastoi *et al.*, 2023) have shown that fully utilizing V2G technology to efficiently utilize the energy storage batteries of parked EVs can bring substantial economic and stability benefits (Hao *et al.*, 2020; Wu *et al.*, 2021). Tan *et al.*, (2024) enhanced the robustness of the distribution network against the uncertainty of distributed power generation by aggregating EVs under the conditions of high penetration of distributed power sources and large-scale grid integration of EVs. Qiu *et al.*, (2024) applied reinforcement learning to propose a multi-agent hierarchical structure for aggregating and scheduling EVs. This not only achieved efficient integration of distributed renewable energy but also met the power adjustment needs of the distribution network through the V2G capability of EVs, thereby improving the stability of the distribution network operation. However, as private assets of users, EVs consider their own interests when responding to the demands of the distribution network (Du *et al.*, 2023; Yin *et al*, 2021). Therefore, Li *et al.*, (2020) and Hui *et al.*, (2022) established a time-of-use pricing incentive strategy to guide EV users to respond to scheduling, achieving the absorption of new energy on the grid side while reducing users' charging costs. Hou *et al.* (2022) further analyzed the price-based and incentive-based demand response mechanisms of EV users, effectively improving the economic benefits of EV aggregators while flattening load fluctuations.

2. Method

The dual-layer partitioned aggregation scheduling architecture for distributed resources in distribution networks is a management and control framework based on the principle of hierarchical and partitioned control, considering the collaborative interaction requirements among different aggregation areas (Li *et al.*, 2024). It involves optimization calculations at both the distribution network layer and the aggregation layer. The distribution network layer manages the overall system and coordinates the scheduling objectives through the aggregation layer, which issues coordinated decisions to the local distributed devices for flexible response.

2.1 The dual-layer partitioned aggregation scheduling structure for distributed resources

The distributed resource partitioned aggregation scheduling architecture for distribution networks addresses issues such as task allocation, resource distribution, and conflict coordination in the overall scheduling of the distribution network through unified management of aggregation layer members by the distribution network control centre. This enables the distribution network to achieve an optimized operating level while allowing distributed devices to implement autonomous management and scheduling under the coordination of the aggregation layer. The distribution network layer, which is the core part of the dual-layer partitioned aggregation scheduling architecture, is responsible for communication with the aggregation layer and generates power control signals to optimize the power consumption and discharge behaviour of each aggregation area based on grid information and data provided by the aggregation layer, such as overall load information, distributed generation status, and EV state of charge (SOC). The aggregation layer acts as a control and negotiation intermediary between the grid and distributed devices. Each aggregation entity collects necessary information from the distributed resources in its area, such as distributed power generation forecasts and energy storage operation status and formulates local control strategies in conjunction with market electricity prices. The basic structure diagram is shown in Figure 1.

2.2 The dual-layer partitioned aggregation optimization scheduling mechanism for distributed resources

In the partitioned aggregation scheduling of distributed resources in distribution networks, the distribution network layer manages the overall operation and economic benefits of the distribution network. It also formulates aggregation partitions based on its own needs and supervises the strategies of the subordinate aggregation layers. The aggregation layer is

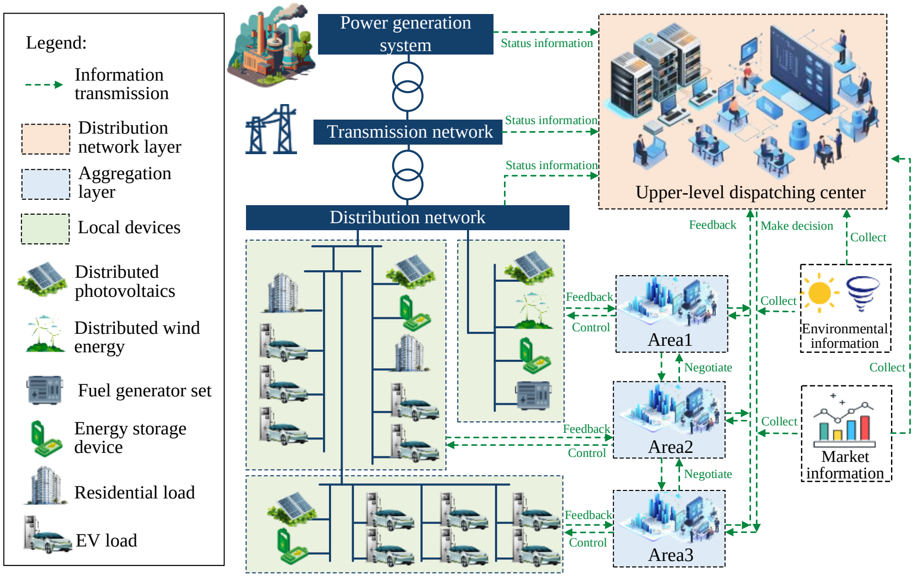

Fig 1. Schematic diagram of hierarchical and partitioned scheduling architecture

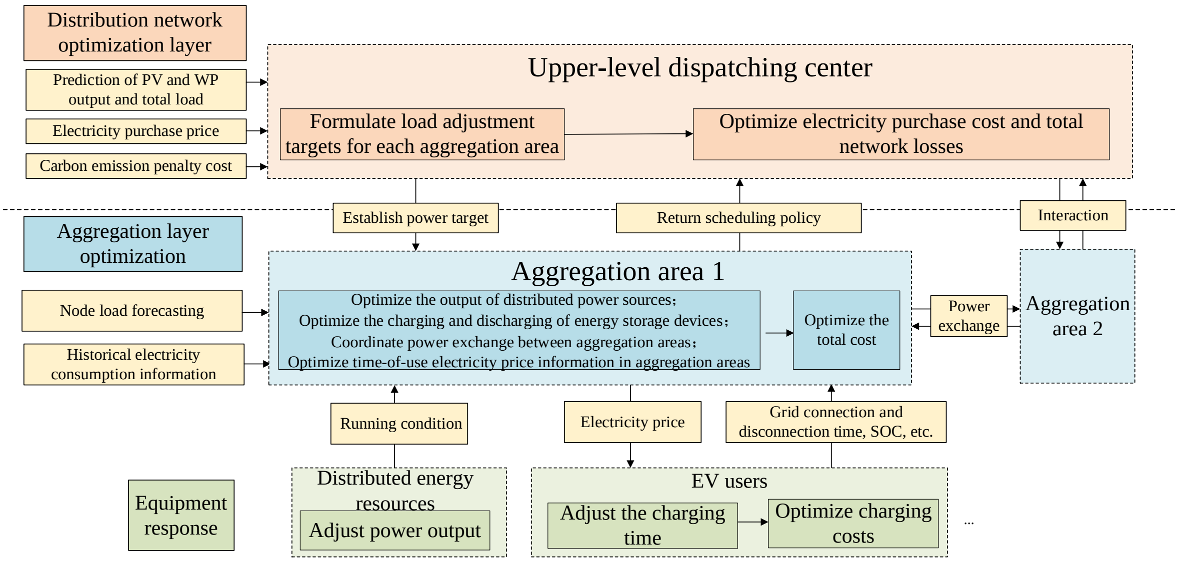

managed by the aggregation entities of each partition, which are responsible for coordinating the operational tasks between upper and lower layers and formulating scheduling strategies to guide and control the controllable distributed resources within the partition. The mechanism is illustrated in Figure 2.

2.3 Low-carbon economic dispatch model for distribution network layer

The optimization of the distribution network layer mainly focuses on the entire distribution network, managing the overall power generation and load operation. On one hand, it needs to ensure the normal operation of the power load in the distribution network. On the other hand, it also needs to take into account its carbon emission responsibilities. The objective function can be defined as:

$$min \quad f_g = \sum_{t=1}^{T}\left(\omega_t^g P_t^g + C_t^g + C_t^c + C_t^{ab}\right) \tag{1}$$

Where, f_g represents the total power generation cost of the distribution network, ω_t^g is the electricity purchase price from external sources during period t, P_t^g is the required power purchase volume of the distribution network during period t, C_t^g is the power generation cost of the operating generation equipment in the distribution network during period t, C_t^c is the carbon emission cost during period t, and C_t^{ab} is the cost of curtailed wind and solar power.

The power generation equipment inevitably emits a large amount of carbon dioxide and other pollutants during the power generation process, and its carbon dioxide emissions are positively correlated with the total output power (Liu *et al.*, 2021), which can be expressed as follows:

$$M_{i,t}^g = R_{\text{gc}} P_{i,t} \tag{2}$$

Where, R_{gc} is the carbon emission coefficient of the power generation equipment, and $P_{i,t}$ is the active power generation of the i-th generator during the time period t. For the carbon dioxide emissions from power generation systems, China currently adopts a free carbon quota allocation scheme based on the baseline method, with the calculation formula as follows:

$$M_{\text{cq}} = \varepsilon_{\text{cq}} \sum_{t=1}^{T}\left(\sum_{i=1}^{N_{\text{gg}}} P_{i,t}\delta_{i,t}^{\text{g}} + \sum_{i=1}^{N_{\text{PV}}} P_{i,t}^{\text{PV}} + \sum_{i=1}^{N_{\text{WP}}} P_{i,t}^{\text{WP}}\right) \tag{3}$$

Where, M_{cq} is the carbon emission quota of the distribution network, ε_{cq} is the baseline carbon emission factor of the region to which the distribution network belongs, $P_{i,t}^{\text{PV}}$ and $P_{i,t}^{\text{WP}}$ are the power generation of distributed photovoltaic and distributed wind power in period t, respectively, and N_{PV} and N_{WP} are the numbers of distributed photovoltaic and distributed wind power generation equipment in the distribution network, respectively.

To further restrict corporate carbon emissions, a stepwise carbon emission cost model is often used to divide carbon emission costs into several intervals. The stepwise carbon emission cost can be expressed as:

$$C_t^{\text{c}} = \begin{cases} -s_t^{\text{c}}\left(M_{\text{gnet},t} - M_{\text{cq}}\right), & M_{\text{gnet},t} < M_{\text{cq}} \\ c_t^{\text{c}}\left(M_{\text{gnet},t} - M_{\text{cq}}\right), & M_{\text{cq}} \le M_{\text{gnet},t} < M_{\text{cq}} + d_{\text{c}} \\ c_t^{\text{c}} d_{\text{c}} + \left(1+k_{\text{c}}\right) c_{\text{c},t}\left(M_{\text{gnet},t} - M_{\text{cq}} - d_{\text{c}}\right), & M_{\text{cq}} + d_{\text{c}} \le M_{\text{gnet},t} < M_{\text{cq}} + 2d_{\text{c}} \\ \left(2+k_{\text{c}}\right) c_t^{\text{c}} d_{\text{c}} + \left(1+2k_{\text{c}}\right) c_t^{\text{c}}\left(M_{\text{gnet},t} - M_{\text{cq}} - d_{\text{c}}\right). & M_{\text{cq}} + 2d_{\text{c}} \le M_{\text{gnet},t} \end{cases} \tag{4}$$

$$M_{\text{gnet},t} = \sum_{i=1}^{N_{\text{gg}}} M_{i,t}^{\text{g}} \tag{5}$$

Where, $M_{\text{gnet},t}$ is the carbon emission of all diesel generators in the distribution network during time period t, c_t^c is the purchase price per unit of carbon quota in the carbon market during period t, s_t^c is the selling price per unit of carbon quota in the carbon market during period t, d_c is the length of the carbon emission interval for the stepwise carbon price, and k_c is the growth coefficient of the carbon trading price for each increase in the carbon emission level.

2.4 Energy interaction strategy between the distribution network layer and the aggregation layer

The low-carbon economic objective of the distribution network layer aims to optimize the scheduling of the total amount of distributed resources in the distribution network. However, due to the large number of distributed resources in actual scheduling, they cannot be directly scheduled by the distribution network layer. Therefore, in operation, it is necessary to leave sufficient scheduling space for the aggregation area's own scheduling, so that the specific energy scheduling within the aggregation area can be autonomously decided by the aggregation entity as much as possible. The energy interaction objective of the aggregation area is:

$$\min \quad f_{\text{loss}} = \sum_{t=1}^{T} \sum_{a,b \in L_l} G_{ab} \left[V_{a,t}^2 + V_{b,t}^2 - 2V_{a,t} V_{b,t} \right] \tag{6}$$

Where, l L_l represents the transmission line branches between different aggregation areas, a and b are the two end nodes corresponding to the same transmission line, $V_{a,t}$ and $V_{b,t}$ are the voltage values of the corresponding nodes, and G_{ab} is the admittance value of the corresponding branch.

For the optimization objectives of the distribution network layer and the interaction objectives of the aggregation areas, the optimization results should include decision-making results and state variables of the distribution network, which can be expressed as:

$$x_t^D = \{P_{i,t}^D, Q_{i,t}^D, V_{i,t}^D, \theta_{i,t}^D\}, x_t^{\text{Dl}} = \{P_{i,t}^{\text{Dl}}, Q_{i,t}^{\text{Dl}}, V_{i,t}^{\text{Dl}}, \theta_{i,t}^{\text{Dl}}\} \tag{7}$$

$$x_t^E = \{\delta_{i,t}^g, \delta_{i,t}^c, P_{i,t}, P_{i,t}^{\text{PV}}, P_{i,t}^{\text{WP}}\}, x_t^{\text{El}} = \left\{\delta_{i,t}^{\text{gl}}, \delta_{i,t}^{\text{cl}}, P_{i,t}^l, P_{i,t}^{\text{lPV}}, P_{i,t}^{\text{lWP}}\right\} \tag{8}$$

Where, x_t^D is the set of state variables after the global optimization of the distribution network layer, and x_t^E is the set of decision variables for the global optimization of the distribution network layer. $P_{i,t}^D$, $Q_{i,t}^D$, $V_{i,t}^D$ and $\theta_{i,t}^D$ are the active power, reactive power, voltage magnitude, and voltage phase angle of node i during time period t, respectively. x_t^{Dl} and x_t^{El} are the corresponding sets of state and decision variables when the objective is defined by Equation (6). Based on the state variables of the distribution network, the distribution network layer will formulate sub-task objectives for the aggregation entities in the aggregation areas, that is:

$$P_{d,t}^Z = max\{\textstyle\sum_{i\in d} P_{i,t}^D, \quad \sum_{i\in d} P_{i,t}^{\text{Dl}}\} \tag{9}$$

$$Q_{d,t}^Z = max\{\textstyle\sum_{i\in d} Q_{i,t}^D, \quad \sum_{i\in d} Q_{i,t}^{\text{Dl}}\} \tag{10}$$

Where, $P_{d,t}^Z$ and $Q_{i,t}^Z$ are the active power and reactive power targets of aggregation area i during time period t, respectively, which are calculated as the sum of the optimized results of all nodes within the area.

In actual operation, the uncertainty of distributed generation output may prevent aggregation areas from meeting their targets. Therefore, different aggregation areas can conduct power transactions through the transmission lines between them. The transaction price should not exceed the price at which the area purchases electricity directly from the external grid.

$$\omega_{d,t}^Z P_{d,t}^B \le \omega_t^g \left[P_{d,t}^B + G_a^Z\left(V_{a,t}^2 + V_{b,t}^2 - 2V_{a,t}V_{b,t}\right)\right] \tag{11}$$

Where, $\omega_{d,t}^Z$ is the electricity purchase price per unit for aggregation area d during time period t from adjacent aggregation areas, $P_{d,t}^B$ is the electricity purchase volume of aggregation area d during time period t. $V_{a,t}$ and $V_{b,t}$ are the voltage values at the two endpoints of the transmission line, and. G_a^Z represents the admittance value from the electricity purchase node a of the aggregation area to the reference node.

2.5 Construction of comprehensive performance indicators for aggregation layer resource aggregation and partitioning

When conducting resource aggregation and partitioning in the aggregation layer, it is necessary to consider the coupling strength between internal and external nodes within the aggregation area, the load-supporting potential of EVs for the distribution network, and the power balance between aggregation areas (Mouli *et al.*, 2017). Therefore, this paper constructs a comprehensive performance indicator for distributed resource aggregation, considering the electrical distance indicator, the dispatchable potential indicator of EVs, and the power balance indicator of aggregated distributed resources under the condition of large-scale EV integration, and proposes a corresponding distributed resource aggregation method. The formulas for each indicator are as follows:

$$s_{ij} = \sqrt{\sum_{n=1}^{N_Q} (d_{in} - d_{jn})^2} \tag{12}$$

$$f_1 = \frac{1}{2m} \sum_i \sum_j (s_{ij} - \frac{k_i k_j}{2m}) \delta(i,j) \tag{13}$$

$$f_{a,d} = E_d^{\text{C}} - E_d^{\text{n}} \tag{14}$$

$$E_d^{\text{C}} = \sum_{ev\_i=1}^{n_d} \min[P_{ev\_i}^{\text{C}}(1+\varepsilon_d)(T_{ev\_i}^{\text{D}} - T_{ev\_i}^{\text{A}})\eta, E_{bat,mev}(1 - SOC_{ar,mev}) / \eta] \tag{15}$$

$$E_d^{\text{n}} = \sum_{ev\_i}^{n_d} (SOC_{ev\_i}^{\text{e}} - SOC_{ev\_i}^{\text{av}}) E_{ev\_i}^{\text{b}} / \eta \tag{16}$$

$$f_{e,d} = \frac{1}{\gamma} \times | P_d^{\text{p}} - \gamma | \tag{17}$$

$$f_2 = w_a f_{a,d}^{'} + w_e f_{e,d}^{'} \tag{18}$$

$$P_{eq,d} = \left| \sum_{t=1}^{T} \left(P_d^{\text{a}}(t) - P_d^{\text{an}}(t) \right) \right| / T \tag{19}$$

$$f_3 = \min \sum_{d=1}^{N_d} \left(P_{eq,d} - \sum_{d=1}^{N_d} P_{eq,d} / N_d \right)^2 \tag{20}$$

$$F = \min\left(\gamma_1 f + \gamma_2 \tau_{\gamma 2} f_2 + \gamma_3 \tau_{\gamma 3} f_3\right) f_c \tag{21}$$

Formulas (12) and (13) represent the electrical distance indicator, where s_{ij} is the electrical distance between nodes i and j (Wang *et al.*, 2022), N_Q is the number of reactive power source nodes, and d_{ij} is the electrical distance between reactive power source node i and controlled node j expressed using electrical sensitivity. k_i is the sum of the edge weights of all branches connected to node i, and m is the sum of the weights of all branches in the electrical network. When nodes i and j are in the same cluster, $\delta(i,j)=1$; otherwise, $\delta(i,j)=0$ .Formulas (14) to (18) represent the dispatchable potential sub-indicators of EVs, where Formula (14) is the dispatchable potential on the user side. E_d^C represents the chargeable energy of EVs in aggregation area d during their dwell time, E_d^n is the energy demand of EVs in aggregation area d, n_d is the number of EVs in aggregation area d, $P_{ev\_i}^C$ is the average acceptable charging power of EVs, $T_{ev\_i}^D$ and $T_{ev\_i}^A$ are the off-grid and on-grid times of EVs, respectively, η is the charging efficiency of EVs, $\text{SOC}_{ev\_i}^e$ is the desired SOC of EVs when they leave the grid, $\text{SOC}_{ev\_i}^{\text{av}}$ is the SOC of EVs when they connect to the grid, and $E_{ev\_i}^b$ is the total battery capacity of EVs. Formula (17) represents the dispatchable potential on the distribution network side, where γ is the desired regulation ratio of the distribution network within the scheduling period, P_d^p s the normalized average of the basic load within the dwell time of EVs, w_a and w_e are the weights of each sub-indicator, and $f_{a,d}^{'}$ and $f_{e,d}^{'}$ are the normalized indices of user EV dispatchable capability and distribution network demand, respectively.

Formulas (19) to (21) represent the power balance indicators for aggregated distributed resources, where $\boldsymbol{P_d^a(t)}$ is the adjustable power capacity of area d during time period t, $\boldsymbol{P_d^{\text{an}}(t)}$ is the required power regulation capacity of area d during time period t, and $\boldsymbol{N_d}$ is the number of divided areas. Formula (21) represents the method for constructing the comprehensive indicator, where $\boldsymbol{\gamma_1}$, $\boldsymbol{\gamma_2}$, and $\boldsymbol{\gamma_3}$ are the weight coefficients of the voltage control sub-indicator, the EV user dispatchable potential sub-indicator, and the distributed resource aggregation power balance sub-indicator, respectively. $\boldsymbol{\tau_{\gamma 2}}$ and $\boldsymbol{\tau_{\gamma 3}}$ are scaling parameters, and $\boldsymbol{f_c}$ is the penalty multiplier for the number of nodes in the aggregation area constraint.

2.6 Economic dispatch objective of distributed resources in the aggregation layer

The aggregation areas in the aggregation layer need to respond to the power targets set by the distribution network layer, while also achieving their own economic objectives through reasonable scheduling. The objective function can be expressed as follows:

$$min \quad f_d^{\mathrm{AD}} = C_d^{\mathrm{dg}} + \sum_{t=1}^{T} \omega_{\mathrm{cg}} \left(\sum_{i=1, i \in d}^{N_{n,d}} P_{i,t}^{\mathrm{AD}} - P_{d,t}^{B} - P_{d,t}^{Z} \right) + \omega_{d,t}^{Z} \sum_{t=1}^{T} P_{d,t}^{B} \tag{22}$$

Where, $P_{i,t}^{\mathrm{AD}}$ is the net active load of each node in aggregation area d after scheduling, ω_{cg} is the reward or penalty price for aggregation area i to complete the active power adjustment target set by the distribution network layer, and C_d^{dg} is the generation cost of the power generation equipment in aggregation area.

The net active load of each node in the aggregation area after scheduling can be defined as:

$$P_{i,t}^{\mathrm{AD}} = P_{i,t}^{l} + P_{i,t}^{\mathrm{EV}} - \left(P_{i,t}^{\mathrm{PV}} + P_{i,t}^{\mathrm{WP}} + P_{i,t} \right) \tag{23}$$

Among them, $P_{i,t}^{l}$ is the base load value of node i during time period t, and $P_{i,t}^{\mathrm{EV}}$ is the charge/discharge power of EV at node i during time period t.

2.7 Economic dispatch objective of distributed resources in the aggregation layer

In general, when electricity prices rise, the demand for electricity correspondingly decreases. To describe the impact of electricity prices on the charging demand of EVs in the distribution network, a price elasticity matrix can be constructed (Liu *et al*., 2020). This matrix reflects the degree of change in user charging demand in response to changes in electricity prices. Each element in the matrix represents the self-price elasticity or cross-price elasticity of charging prices during that time period, as shown in Formula (24).

$$\mathrm{E}^{\mathrm{V}} = \begin{bmatrix} e_{11} & e_{12} & \cdots & e_{1T} \\ e_{21} & e_{22} & \cdots & e_{2T} \\ \vdots & \vdots & \ddots & \vdots \\ e_{T1} & e_{T2} & \cdots & e_{TT} \end{bmatrix} \tag{24}$$

According to Reference (Liu D N *et al*., 2020), the charging demand response of EV users can be expressed as:

$$\begin{bmatrix} \Delta E_{i,t_1}^{\mathrm{C}} / E_{i,t_1}^{\mathrm{V}} \\ \Delta E_{i,t_2}^{\mathrm{C}} / E_{i,t_2}^{\mathrm{V}} \\ \vdots \\ \Delta E_{i,t_T}^{\mathrm{C}} / E_{i,t_T}^{\mathrm{V}} \end{bmatrix} = \frac{1}{T} \times \mathrm{E}_i^{\mathrm{V}} \begin{bmatrix} \Delta P_{t_1}^{\mathrm{cp}} / P_{t_1}^{\mathrm{cp}} \\ \Delta P_{t_2}^{\mathrm{cp}} / P_{t_2}^{\mathrm{cp}} \\ \vdots \\ \Delta P_{t_T}^{\mathrm{cp}} / P_{t_T}^{\mathrm{cp}} \end{bmatrix} \tag{25}$$

Among them, E_{i,t_m}^{V} is the charging demand of EV user i during time period t_m, $P_{t_m}^{\mathrm{cp}}$ is the initial charging price during time period t, $\Delta P_{t_1}^{\mathrm{cp}}$ is the difference between the actual price and the initial charging price, and $\Delta E_{i,t_m}^{C}$ is the adjustment amount of the charging power.

Mapping the time period to the peak period (p), off-peak period (o), and valley period (v), the user's charging price elasticity matrix under time-of-use pricing is:

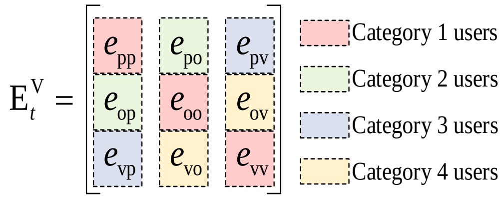

Fig 3. Classification of four types of users

$$\mathrm{E}_i^{\mathrm{V}} = \begin{bmatrix} e_{\mathrm{pp}} & e_{\mathrm{po}} & e_{\mathrm{pv}} \\ e_{\mathrm{op}} & e_{\mathrm{oo}} & e_{\mathrm{ov}} \\ e_{\mathrm{vp}} & e_{\mathrm{vo}} & e_{\mathrm{vv}} \end{bmatrix} \tag{26}$$

2.8 Economic dispatch objective of distributed resources in the aggregation layer

After the aggregation entity formulates the peak, valley, and off-peak time-of-use electricity prices based on the historical charging behavior of EVs, according to the load shifting among peak, off-peak, and valley periods during their parking time, EV users can be roughly divided into four categories: peak-valley users, peak-off-peak users, valley-off-peak users, and peak-valley-off-peak users (Li *et al*., 2022).

- Type1: Peak-Valley Charging Users: EV users connect to the distribution network for charging only during the time periods corresponding to peak, off-peak, or valley electricity prices.
- Type2: Peak-Off-Peak Users: EV users connect to the distribution network for charging during both peak and off-peak periods but not during valley periods.
- Type3: Valley-Off-Peak Users: EV users connect to the distribution network for charging during both valley and off-peak periods, and the total chargeable energy in these two periods can fully cover the user's responsive energy demand.
- Type4:Peak-Off-Peak-Valley Users: EV users connect to the distribution network for charging during all three periods (peak, off-peak, and valley), but the total charging energy in the valley and off-peak periods cannot fully cover the user's responsive energy demand.

For the four types of EV users, the scheduling strategies for each type can be shown in Figure 4. Among them, since the total charging volume of Type 4 EV users during the valley and off-peak periods cannot cover the user's responsive power demand, and the adjustment space within the range of meeting their own power needs is relatively small, it is necessary to prioritize their charging during the valley and off-peak periods to fully respond to the load adjustment requirements of the distribution network. For Type 1 EV users, since their load shifting space is relatively limited in the time dimension, their charging load should be adjusted immediately after that of Type 4 EV users, so that they can charge as close as possible to the peak or valley load points during the peak or valley time periods. For Type 2 and Type 3 EV users, they can be scheduled separately within the corresponding time periods.

2.9 Constraints

The above models all need to meet various constraints for the normal operation of the distribution network.

(1) Security constraints

Voltage Constraints

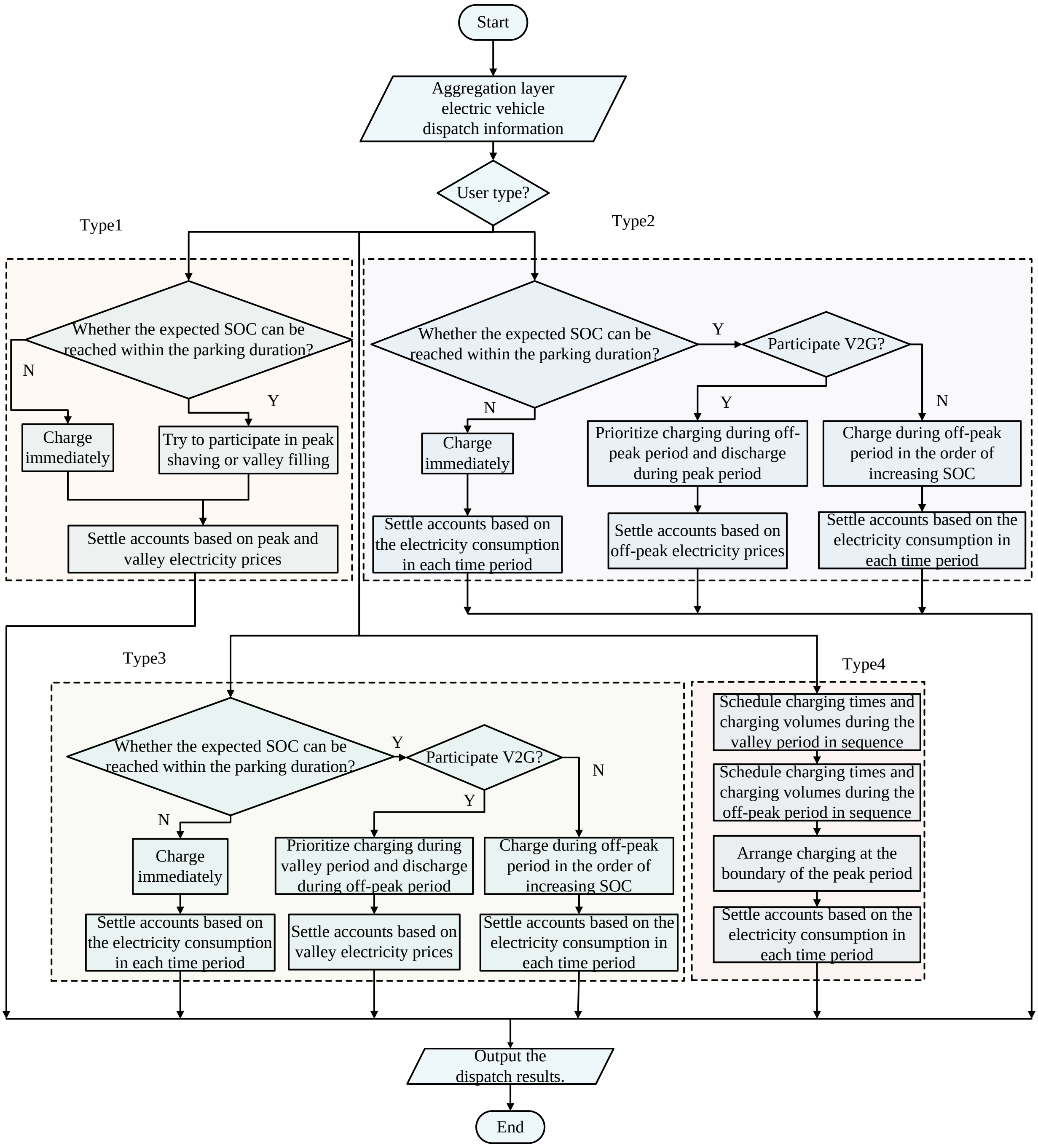

Fig 4. Scheduling process for four types of EV users

$$V_i^{\min} \le V_{i,t} \le V_i^{\max} \tag{27}$$

Where, $V_{i,t}$ is the voltage magnitude of node i during time period t, V_i^{min} and V_i^{max} are the minimum and maximum allowable voltage magnitudes for all nodes in the distribution network.

Line Capacity Constraints

$$I_{ij,t} \le I_{ij}^{max} \tag{28}$$

Where, $I_{ij,t}$ is the current value of the branch from node i to node j during time period t, and I_{ij}^{max} is the maximum allowable current value of the branch.

Node Power Constraints

$$P_i^{\min} \le P_{i,t} \le P_i^{\max} \tag{29}$$

$$Q_i^{\min} \le Q_{i,t} \le Q_i^{\max} \tag{30}$$

Where, P_i^{min} and P_i^{max} are the minimum and maximum limits of the active power at node i, respectively; Q_i^{min} and Q_i^{max} are the minimum and maximum limits of the reactive power at node i, respectively.

(2) Power flow balance constraints

$$P_t^{\mathrm{g}} + P_{i,t} + P_{i,t}^{\mathrm{PV}} + P_{i,t}^{\mathrm{WP}} = P_{i,t}^{\mathrm{l}} + V_{i,t} \sum_{j=1}^{N_{\mathrm{n}}} V_{j,t} \left(G_{ij} \cos\theta_{ij,t}^{\mathrm{n}} + B_{ij} \sin\theta_{ij,t}^{\mathrm{n}} \right) \tag{31}$$

$$Q_t^{\mathrm{g}} + Q_{i,t}^{\mathrm{PV}} + Q_{i,t}^{\mathrm{WP}} + Q_{i,t}^{\mathrm{C}} = Q_{i,t}^{\mathrm{l}} + V_{i,t} \sum_{j=1}^{N_{\mathrm{n}}} V_{j,t} \left(G_{ij} \sin\theta_{ij,t}^{\mathrm{n}} + B_{ij} \cos\theta_{ij,t}^{\mathrm{n}} \right) \tag{32}$$

Where, $P_{i,t}^{l}$ and $Q_{i,t}^{l}$ are the magnitudes of the active and reactive power loads connected to node i during time period t, $\boldsymbol{Q}_{i,t}^{\mathrm{PV}}$, and $\boldsymbol{Q}_{i,t}^{\mathrm{WP}}$ are the reactive power outputs of the photovoltaic generation, wind power generation, and reactive power compensation devices at node i respectively, $\boldsymbol{N_n}$ is the number of nodes in the distribution network; $\boldsymbol{\theta}_{ij,t}^{n}$ are the voltage phase angles of nodes i and j, $\boldsymbol{G_{ij}}$ and $\boldsymbol{B_{ij}}$ are the conductance and susceptance of the branch between nodes i and j.

(3) Reactive power compensation constraints

$$Q_{\mathrm{C},i}^{\min} \le Q_{\mathrm{C},i,t} \le Q_{\mathrm{C},i}^{\max} \tag{33}$$

$$Q_{\mathrm{C},i,t} = k_{i,t}\Delta Q_{\mathrm{C},i}, k_{i,t} = 0,1,2,\ldots,N_{\mathrm{C},i} \tag{34}$$

Where, $\boldsymbol{Q}_{\mathrm{C},i}^{min}$ and $\boldsymbol{Q}_{\mathrm{C},i}^{max}$ are the lower and upper limits of the reactive power output of the reactive power compensation device at node i, respectively, $\boldsymbol{k_{i,t}}$ is the number of reactive power compensation devices put into operation at node i during time period t, $\boldsymbol{N_{\mathrm{C},i}}$ is the total number of reactive power compensation devices equipped at node i, $\boldsymbol{\Delta Q_{\mathrm{C},i}}$ is the reactive power compensation capacity of each reactive power compensation device at node i.

3. Results and analysis

3.1 Data description

The case study in this chapter is based on the IEEE 33-node standard test system with a base voltage of 12.66 kV for analysis. The modeling is conducted on the MATLAB 2022a platform using YALMIP, and the optimization problems are solved using the CPLEX and GUROBI solvers. The temporal distribution of base loads at each node is set according to (Xu *et al.*, 2019). The EV data are generated based on the scheme in Reference (Xu *et al.*, 2012), with a total of 3,000 vehicles. The parameters of the power generation equipment are set according to (Tao *et al.*, 2023). Other distributed energy resource parameters are set based on (Hou *et al.*, 2020; Cai *et al.*, 2012; Li *et al.*, 2024). A total of 12 photovoltaic (PV) systems, 1 small wind turbine (PW), and 1 diesel generator (GT) are connected to the network. The connection locations and upper limits of active power output are shown in Table 1.

The carbon trading and renewable energy waste penalty parameters are set according to (Cheng *et al.*, 2022; Zhao *et al.*, 2022), that is: the base price of carbon trading is 200 yuan/t, the length of the carbon emission interval for the stepwise carbon price is 50t, the growth rate of the carbon price is 25%, the carbon emission quota coefficient is 0.7 kg/kWh, the proportion of thermal power in external electricity purchases is 47.6% (National Energy Administration, 2024), and the unit costs of curtailed wind and solar power are 0.1 yuan/kWh.

The base charging electricity price for the aggregation area is set according to (Liu *et al.*, 2021). The floating proportion of the elastic electricity price does not exceed 50%. The peak and

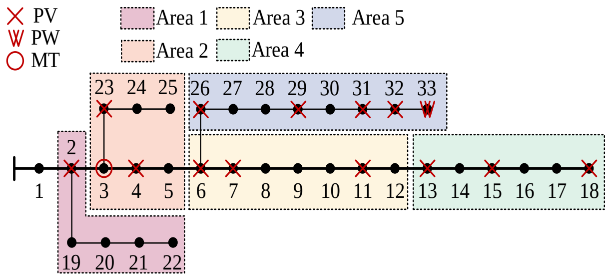

valley electricity prices are set based on the capacity electricity price in Jiangsu Province. The external electricity purchase price is 32 yuan/kVA*month. According to the time-of-use electricity price formulation in (Wang *et al.*, 2023) and the impact of time-of-use electricity prices on active power in different periods, the parameters of the electricity price elasticity matrix in Equation are fitted using SPSS software (Chen *et al.*, 2020), resulting in the corresponding electricity price elasticity matrix as follows:

$$\mathrm{E}_i^{\mathrm{V}} = \begin{bmatrix} e_{\mathrm{pp}} & e_{\mathrm{po}} & e_{\mathrm{pv}} \\ e_{\mathrm{op}} & e_{\mathrm{oo}} & e_{\mathrm{ov}} \\ e_{\mathrm{vp}} & e_{\mathrm{vo}} & e_{\mathrm{vv}} \end{bmatrix} = \begin{bmatrix} -0.21 & 0.04 & 0.07 \\ 0.02 & -0.16 & 0.06 \\ 0.01 & 0.01 & -0.11 \end{bmatrix} \tag{35}$$

3.2 Aggregation layer partitioning results and analysis

To better explore the impact of EV aggregation on the aggregation of distributed resources in the distribution network, this paper adjusts the weight of the EV dispatchable potential sub-indicator to a higher level, fully considering the scenario of EV dispatchable potential. The weights of each sub-indicator are as follows: α=0.5, β=0.9, γ=0.4 (LI Hao *et al.*, 2022). The partitioning results are shown in Figure 5.

This paper selects Aggregation Area 2 and Aggregation Area 5 for analysis, as shown in Figure 6 (a) and Figure 6 (b). The EVs in each aggregation area can provide sufficient power for peak shaving and valley filling to meet the demands of the aggregation areas. In some time periods, the load adjustment demands have already approached the limits of the EVs' peak shaving and valley filling capabilities. For example, in Aggregation Area 2, the peak shaving and valley filling demands at 5:00 and 7:00 have reached 87.0% and 83.4% of the EVs' peak shaving and valley filling capabilities, respectively. In Aggregation Area 5, the valley filling demand at 14:00 has reached 89.1% of its capability. The proportion of peak shaving and valley filling demands in these aggregation areas relative to the EVs' capabilities is also relatively high. Therefore, under the influence of the EVs' bilateral dispatchable potential sub-indicator, the allocation of EVs' peak shaving and valley filling capabilities has already been relatively balanced, not only does it effectively utilize the energy storage potential of electric vehicles, but it also significantly optimizes the load curve of the

Table1
Connection nodes and upper limits of active power output for distributed energy resources

Node	$P_{\mathrm{DG},i}^{\max}$ /kW	Type	Node	$P_{\mathrm{DG},i}^{\max}$ /kW	Type	Node	$P_{\mathrm{DG},i}^{\max}$ /kW	Type
2	550	PV	13	200	PV	29	400	PV
4	200	PV	15	100	PV	31	250	PV
6	300	PV	18	100	PV	32	100	PV
7	200	PV	23	650	PV	33	200	PW
11	200	PV	26	350	PV	3	200	GT

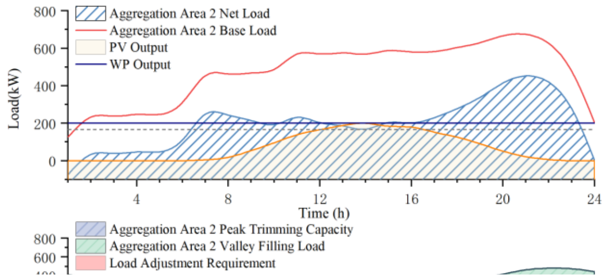

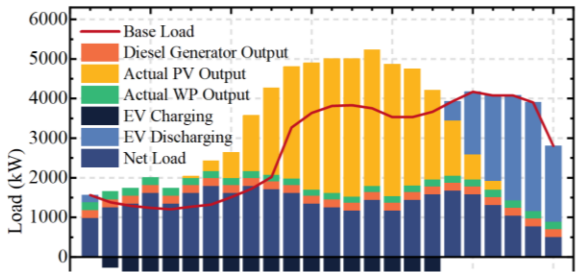

entire power grid, thereby enhancing the stability and economic efficiency of its operation. By reasonably scheduling the charging and discharging behavior of electric vehicles, excessive concentration of grid load is avoided, and the accommodation capacity for renewable energy is further improved, achieving comprehensive benefits in multiple aspects (Feng *et al*., 2021).

3.3 Optimization dispatch results and analysis of the distribution network laye

The optimal output of distributed resources from a global perspective of the distribution network layer is shown in Figure 7, and the daily electricity costs before and after optimization are shown in Table 2. From the scheduling results, the distribution network layer optimizes all distributed resources in the distribution network from a global perspective. Compared to the aggregation layer's optimization, it's limited by its direct data collection from distributed devices and end-to-end negotiation with electric vehicles. It can only optimize the output of distributed power sources and the charging/discharging of electric vehicles based on the total configuration and overall operation probability of distributed resources, without direct control over each unit or vehicle's status. The figure shows that with industrial and commercial loads added, the distribution network has two power consumption peaks: 11:00-16:00 and 19:00-23:00. The high-capacity distributed photovoltaic power generation in the distribution network effectively supports the first peak, while scheduling electric vehicle V2G during the second peak can cut the peak, shift charging to low-demand and photovoltaic output peak times, avoiding peak overlap and boosting renewable energy consumption. This peak load reduction lowers the single-day purchase cost from 6,274.51 yuan to 2,258.82 yuan and the daily operation cost from 11,551.88 yuan to 6,220.84 yuan, delivering good economic benefits.

Figure 8 presents the output of distributed energy resources after distribution network layer optimization. As shown in Figure 8, distributed photovoltaic and wind power generation units both run at maximum output after optimization. Photovoltaic output rises during daytime with sufficient sunlight, closely following the maximum output curve, indicating efficient use of light resources. Wind power generation is relatively stable,

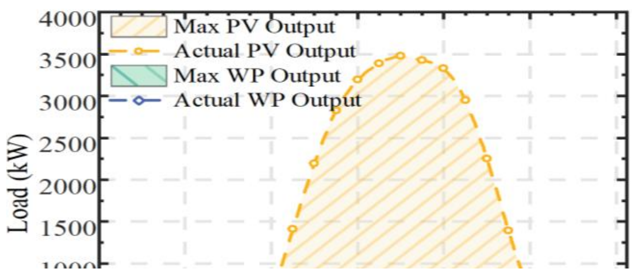

Table 2
Comparison of daily electricity costs before and after optimization of the distribution network layer
Unit: Yuan

	External electricity purchase costs	Diesel generation cost	Cost of curtailed wind and solar power	Carbon emission cost	Total cost
Before optimization	6274.51	3288.6	632.60	1356.16	11551.88
After optimization	2258.82	3288.6	0	673.42	6220.84

with output fluctuating within a range but staying close to the maximum, reflecting effective use of wind resources.

3.4 Optimization dispatch results and analysis of distributed resources in the aggregation layer

To better verify the effects of the scheduling strategy for distributed resources in the aggregation layer considering the price-based demand response of EVs) and the implementation of V2G by EV users, Aggregation Area 5, which has a diverse range of distributed resources, is selected for simulation analysis. The effects of distributed resource scheduling before and after optimization in this aggregation area are shown in Figures 9 (a) and (b).

Figure 9(a) shows that the aggregation area has a substantial amount of distributed renewable energy resources, which can basically meet the base load demand within the area from 8:00 to 19:00 (Zhao *et al*., 2022). Figure 9 (b) indicates that the peak output of distributed renewable energy is concentrated between 9:00 and 19:00. During this period, although the aggregation area needs to purchase some load from the upper-level nodes, it is within the task targets set by the optimized distribution network layer, and there is no need to pay additional electricity purchase fees to adjacent aggregation areas. For the base load and EV charging load in other time periods, the output of distributed photovoltaic and wind power is no longer sufficient to meet the demand. Therefore, some V2G users need to discharge to support the load demand, thereby achieving active power balance within the aggregation area.

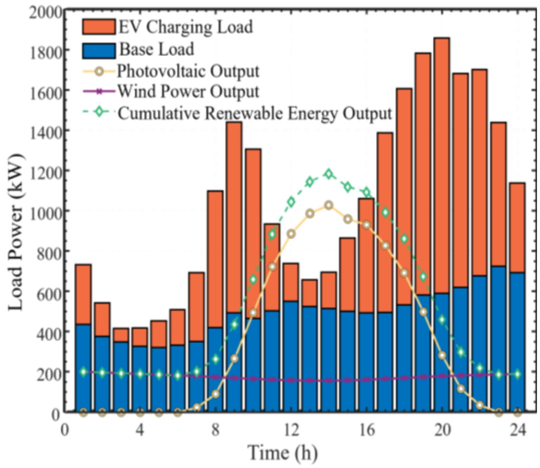

(a) Before optimization dispatch

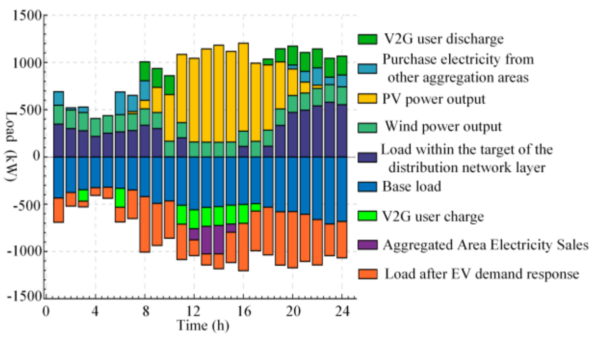

(b) After optimization dispatch

Fig 9. Operating status of distributed resources in the aggregation layer before and after optimization dispatch

4. Conclusion

Simulation results show that the bilevel zonal dispatch strategy for EV demand response proposed in this paper significantly improves the economic and low - carbon performance of power systems. In the distribution network layer, through global resource optimization and cross - area energy interaction strategies, the system's daily operating cost has been reduced from 11,551.88 yuan before optimization to 6,220.84 yuan, a decrease of 46.1%. At the same time, by coordinating the output of distributed photovoltaic and wind power generation, peak shaving and valley filling are effectively achieved, reducing the peak - to - valley difference and increasing renewable energy utilization. In the aggregation layer, a user classification scheduling mechanism based on price elasticity fully taps the flexibility potential of EVs. Under the premise of meeting users' charging needs, it guides their charging and discharging behavior to match the renewable energy output curve, significantly improving local new energy consumption within the aggregation area without over - regulation. Moreover, the zonal aggregation plan, which comprehensively considers electrical distance, EV dispatchability, and power balance, has realized efficient resource synergy and proved the model's practicality in complex scenarios.

Author Contributions: Zhenya Ji: conceptualization, supervision, formal analysis, writing-review and editing, validation. Yuyang Zhang: conceptualization, methodology, review original draft, editing. Zheng Wang: review and editing. Lulu Liu: supervision, writing-reviewing and editing. Hao Li: review and editing. All authors have read and agreed to the published version of the manuscript.

Funding: The research presented in this paper is financially supported by National Natural Science Foundation of China (No. 52107100).

Conflicts of Interest: The authors declare no conflict of interest.

References

Adham, M., Keene, S., & Bass, R. B. (2025). Distributed Energy Resources: A Systematic Literature Review. *Energy Reports*, *13*, 1980-1999.https://www.sciencedirect.com/science/article/pii/S2352484725000265

Ahsan, F., Dana, N. H., Sarker, S. K., Li, L., Muyeen, S. M., Ali, M. F., ... & Das, P. (2023). Data-driven next-generation smart grid towards sustainable energy evolution: techniques and technology review. *Protection and Control of Modern Power Systems*, *8*(3), 1-42.https://pcmp.springeropen.com/articles/10.1186/s41601-023-00319-5

Cai, G., Kong, L., Yang, D., Pan, C., & Sun, Z. L. (2012). Research on modelling and operation characteristics analysis of large-scale wind & light complementary electricity-generating system. *Power System Technology*, *36*(1), 65-71.http://www.dwjs.com.cn/VEe8oYQ2cpp4CLHK1PAH1vUzo0qz87AWscLp5Vsngd4%3D?encrypt=1

Zhong, C., Yi, L., Tao, Z., Qiang, X., & Puliang, D. (2020). Optimal time-of-use charging pricing strategy of EVs considering mobile characteristics. *Electric Power Automation Equipment*, *40*(4), 96-102.http://www.aeps-info.com/aeps/article/abstract/20220930003?st=search

Chen, D., Liu, F., & Liu, S. (2022). Optimization of virtual power plant scheduling coupling with P2G-CCS and doped with gas hydrogen based on stepped carbon trading. *Power System Technology*, *46*(6), 2042-2054.https://doi.org/10.13335/j.1000-3673.pst.2021.2177

Du, W., Ma, J., & Yin, W. (2023). Orderly charging strategy of electric vehicle based on improved PSO algorithm. *Energy*, *271*, 127088.https://www.sciencedirect.com/science/article/pii/S0360544223004826

Changsen, F. E. N. G., Jiang, S. H. E. N., & Chongjuan, Z. H. A. O. (2021). Cooperative game-based coordinated operation strategy of smart energy community. *Electric Power Automation Equipment*, *41*(4), 85-93. https://www.epae.cn/dlzdhsb/ch/reader/view_abstract.aspx?file_no=202104012&flag=1

Shijie, F. E. N. G., Tao, L. I. U., Sa, P. A. N., Zhenghao, C. H. E. N., & Qing, W. A. N. G. (2021). Coordinated charging strategy for electric vehicles based on hierarchical optimization. *Journal of Electrical Engineering*, *16*(3), 137-144. http://www.cjeecmp.cn/CN/10.11985/2021.03.019

Mousa, H. H., Mahmoud, K., & Lehtonen, M. (2024). A comprehensive review on recent developments of hosting capacity estimation and optimization for active distribution networks. *IEEe Access*, *12*, 18545-18593. https://ieeexplore.ieee.org/document/10415382

Hao, L., Wang, G., Wang, H., Huang, M., & Xu, X. Y. (2020). Day-ahead scheduling strategy of distribution network considering electric vehicle-to-grid auxiliary service. *Automation of Electric Power Systems*, *44*(14), 35-43. http://www.aeps-info.com/aeps/article/abstract/20190911002?st=search

Hou, H., Tand, J., Wang Y. and Hu, P. (2022). Long-time-scale charging and discharging scheduling of electric vehicles under joint price and incentive demand response. *Automation of Electric Power Systems*, *46*(15), 46-55. http://www.aeps-info.com/aeps/article/abstract/20220201001?st=search

Hou, H., Xue, M., Xu, Y., Deng, X., Xu, T.,& Cui, R. (2020). Multi-objective economic dispatch of a microgrid considering electric vehicle and transferable load. *Applied Energy*, *262*, 114489. https://www.sciencedirect.com/science/article/abs/pii/S0306261920300015

Huang, H., Li, Y., & Liu, H. (2023). Collaborative optimization strategy of source-grid-load-energy storage based on improved Nash-Q equilibrium transfer algorithm. *Electric Power Automation Equipment*, *43*(8), 71-77. https://www.epae.cn/dlzdhsb/ch/reader/view_abstract.aspx?file_no=202308010&flag=1

Hou, H., Tang, J., Wang, Y., Wang, F., & Hu, P. (2022). Long-time-scale charging and discharging scheduling of electric vehicles under joint price and incentive demand response. *Automation of Electric Power Systems*, *46*(15), 46-55. http://www.aeps-info.com/aeps/article/abstract/20220201001?st=search

Kempton, W., & Tomić, J. (2005). Vehicle-to-grid power implementation: From stabilizing the grid to supporting large-scale renewable energy. *Journal of power sources*, *144*(1), 280-294. https://www.sciencedirect.com/science/article/abs/pii/S0378775305000212

Hao, L. I., Zhenya, J. I., Xiaofeng, L. I. U., Shiwei, Z. H. A. N. G., & Yuqing, B. A. O. (2022). Electric vehicle priority dispatch policy based on comprehensive dispatchable potential assessment model [J]. *Integrated Intelligent Energy*, *44*(11), 1-11. https://www.hdpower.net/CN/10.3969/j.issn.2097-0706.2022.11.001

Li, J., Zhang, Y., Chen, C., Wang, X., Shao, Y., Zhu, X., & Li, C. (2024). Two-Stage Planning of Distributed Power Supply and Energy Storage Capacity Considering Hierarchical Partition Control of Distribution Network with Source-Load-Storage. *Energy Engineering*, *121*(9). https://www.sciencedirect.com/org/science/article/pii/S0199859524001167

Li, S. H., Li, L. L., Tao, D. W., & Ding, Z. (2024). Optimization Method to the Location and Capacity of Backup Cables in Wind Farm With Doubly-fed Induction Generator. *Power System Technology*, *48*(3), 1125-1132. http://www.dwjs.com.cn/Mv5msuBlJAqERWutSrIms_rGxhUCHfCGHp9YOfgLC4Y_j8rpIIlNXSaDJ7KD8s2I?encrypt=1

Li, X. S., Chen, M. R., Cheng, S. (2020). Research on Optimal Scheduling Strategy of Microgrid with Electric Vehicles Based on Dual Incentive Cooperative Game. High *Voltage Engineering*, *46*(7), 2286-2295. http://hve.epri.sgcc.com.cn/MGWd9quGngCBNY4_vz96klLUgrD21BpjhL1YBzc%2BAzlJjM_QsleVCDl4IKOtDb4B?encrypt=1

Dunnan, L. I. U., Erfeng, X. U., Mingguang, L. I. U., Baozhong, Z. H. O. U., & Yuhang, Y. I. N. G. (2020). TOU pricing method for park considering local consumption of distributed generator. *Automation of Electric Power Systems*, *44*(20), 19-28. http://www.aeps-info.com/aeps/article/abstract/20200123004?st=search

Liu, H. T., Chen, J., & Zhu, X. (2021). An incentive strategy of residential peak-valley price based on price elasticity matrix of demand. *Power System Protection and Control*, *49*(5), 116-123. https://www.dlbh.net/dlbh/ch/reader/view_abstract.aspx?file_no=20210513&flag=1

Liu, Z., Chen, X. Y., & Zou, S. Y. (2021). Optimal Capacity Configuration Method for Wind-Photovoltaic-Pumped-Storage System Considering Carbon Emission. *Automation of Electric Power Systems*, *45*(22), 9-18. http://www.aeps-info.com/aeps/article/abstract/20210221003?st=search

Luo, E., Cong, P., Lu, H., & Li, Y. (2020). Two-stage hierarchical congestion management method for active distribution networks with multi-type distributed energy resources. *IEEE Access*, *8*, 120309-120320.https://ieeexplore.ieee.org/document/9127892

Mastoi, M. S., Zhuang, S., Munir, H. M., Haris, M., Hassan, M., Alqarni, M., & Alamri, B. (2023). A study of charging-dispatch strategies and vehicle-to-grid technologies for electric vehicles in distribution networks. *Energy Reports*, *9*, 1777-1806. https://www.sciencedirect.com/science/article/pii/S2352484722027408

Mouli, G. R. C., Kefayati, M., Baldick, R., & Bauer, P. (2017). Integrated PV charging of EV fleet based on energy prices, V2G, and offer of reserves. *IEEE Transactions on Smart Grid*, *10*(2), 1313-1325.https://ieeexplore.ieee.org/document/8068996

Naqash, M. T., Aburamadan, M. H., Harireche, O., AlKassem, A., & Farooq, Q. U. (2021). The potential of wind energy and design implications on wind farms in Saudi Arabia. *International Journal of Renewable Energy Development*, *10*(4), 839. https://doi.org/10.14710/ijred.2021.38238

Nguyen, T. T. M., Khoa, P. N. D., & Huynh, N. A. (2022). Electrical energy management according to pricing policy: a case in Vietnam. *International Journal of Renewable Energy Development*, *11*(3), 851-862.https://ijred.cbiore.id/index.php/ijred/article/view/46302

Qiu, D., Wang, Y., Sun, M., & Strbac, G. (2022). Multi-service provision for electric vehicles in power-transportation networks towards a low-carbon transition: A hierarchical and hybrid multi-agent reinforcement learning approach. *Applied Energy*, *313*, 118790. https://www.sciencedirect.com/science/article/pii/S0306261922002379

Shan, Y., Ma, L., & Yu, X. (2023). Hierarchical control and economic optimization of microgrids considering the randomness of power generation and load demand. *Energies*, *16*(14), 5503.https://www.mdpi.com/1996-1073/16/14/5503

Tan, B., Chen, S., Liang, Z., Zheng, X., Zhu, Y., & Chen, H. (2024). An iteration-free hierarchical method for the energy management of multiple-microgrid systems with renewable energy sources and electric vehicles. *Applied energy*, *356*, 122380. https://www.sciencedirect.com/science/article/pii/S0306261923017440

Zhang, T., Liu, K., Tao, R., Wang, Q., & Huang, M. (2023). Integrated energy system optimization considering thermal inertia and CSP station. *Electric Power Construction*, *44*(1), 109-117. https://doi.org/10.12204/j.issn.1000-7229.2023.01.013

Teng, C., Ji, Z., Yan, P., Wang, Z., & Ye, X. (2024). Orderly charging strategy for electric vehicles based on multi-level adjustability. *International Journal of Renewable Energy Development*, *13*(2), 245-255. https://doi.org/10.61435/ijred.2024.60053

Tian, X., Zha, H., Tian, Z., Lang, G., & Li, L. (2024). Carbon emission reduction capability assessment based on synergistic optimization control of electric vehicle V2G and multiple types power supply. *Energy Reports*, *11*, 1191-1198. https://www.sciencedirect.com/science/article/pii/S2352484724000039

Tippichai, A., Teungchai, K., & Fukuda, A. (2023). Energy demand modeling for low carbon cities in Thailand: A case study of Nakhon Ratchasima province. *International Journal of Renewable Energy Development*, *12*(4), 655-665. https://ijred.cbiore.id/index.php/ijred/article/view/53211

Shouxiang, W. A. N. G., Hanzhang, W. A. N. G., & Qianyu, Z. H. A. O. (2023). Optimization method of time-of-use electricity price for improving photovoltaic hosting capacity of distribution network. *Automation of Electric Power Systems*, *47*(10), 38-46. http://www.aeps-info.com/aeps/article/abstract/20220930003?st=search

Wang, Z. P., & Liang, Z. W. (2022). Big Data Research Report on New Energy Vehicles in China. Machinery Industry Press. https://xueshu.baidu.com/usercenter/paper/show?paperid=1t6d08b0at530c901y2800u08x699741&site=xueshu_se&hitarticle=1

Wu, Y., Wu, Y., Guerrero, J. M., & Vasquez, J. C. (2021). A comprehensive overview of framework for developing sustainable energy internet: From things-based energy network to services-based management system. *Renewable and Sustainable Energy Reviews*, *150*, 111409. https://www.sciencedirect.com/science/article/pii/S1364032121006936

Chengsi, X., Shufeng, D. O. N. G., & Jiaqi, Z. (2019). Description method of radial constraints for distribution network based on disconnection condition of power supply loop. *Automation of Electric Power Systems*, *43*(20), 82-89. http://www.aeps-info.com/aeps/article/abstract/20180904011?st=search

Xu, Z., Hu, Z., Song, Y., Luo, Z., Zhan, K., & Shi, H. (2012). Coordinated charging of plug-in electric vehicles in charging stations. *Automation of Electric Power Systems*, *36*(11), 38-43. http://www.aeps-info.com/aeps/article/abstract/201103033?st=search

Yang, K., Zhang, Q., Wang, G., Li, H., & McLellan, B. (2024). A new model for comprehensively evaluating the economic and environmental effects of vehicle-to-grid (V2G) towards carbon neutrality. *Journal of Energy Storage*, *98*, 113067. https://www.sciencedirect.com/science/article/pii/S2352152X24026537

Yin, W., Ming, Z., & Wen, T. (2021). Scheduling strategy of electric vehicle charging considering different requirements of grid and users. *Energy*, *232*, 121118. https://www.sciencedirect.com/science/article/pii/S0360544221013669

Dongmei, Z., Haoxiang, W., & Ran, T. (2022). Multi-source coordinated robust economic scheduling strategy of DC cross regional interconnected grid with nuclear power and carbon capture units. *Power System Technology*, *46*(10), 4064-4077. http://www.dwjs.com.cn/Mv5msuBlJAqERWutSrIms_rGxhUCHfCGHp9YOfgLC4arHSyRG4Y0cI6SId6Q1QNj?encrypt=1

Zhao, J., Tang, Z., Wang, G., Chen, Y., Wang, W., Chen, K., & Wu, Y. (2022). Operation characteristics of user-side resources with energy storage function. *Integrated Intelligent Energy*, *44*(2), 8-14. https://www.hdpower.net/CN/10.3969/j.issn.2097-0706.2022.02.002

Pengzhen, Z. H. A. O., Ning, X. I. E., Jiamin, Y. I. N., & Chengmin, W. (2023). Centralized-distributed pattern of distribution network and its hierarchical partition method adapting to development trend of new power system [J]. *Smart Power*, *51*(1), 94-100.http://zhdlqk.sn.sgcc.com.cn:19001/#/digest?ArticleID=5630